Journal of Molecular and Cellular Cardiology 110 (2017) 61–69

Contents lists available at ScienceDirect

Journal of Molecular and Cellular Cardiology

journal homepage: www.elsevier.com/locate/yjmcc

# D242N, a $K_V$7.1 LQTS mutation uncovers a key residue for $I_{Ks}$ voltage dependence

Cristina Moreno [a,1,2], Anna Oliveras [b,2], Chiara Bartolucci [c], Carmen Muñoz [d], Alicia de la Cruz [a], Diego A. Peraza [a], Juan R. Gimeno [d], Mercedes Martín-Martínez [e], Stefano Severi [c], Antonio Felipe [b], Pier D. Lambiase [f], Teresa Gonzalez [a,*], Carmen Valenzuela [a,*]

[a] Instituto de Investigaciones Biomédicas Alberto Sols CSIC-UAM, Madrid, Spain
[b] Molecular Physiology Laboratory, Dpt. de Bioquímica i Biologia Molecular, Institut de Biomedicina (IBUB), Universitat de Barcelona, Spain
[c] Computational Physiopathology Unit, Dpt. of Electrical, Electronic and Information Engineering "Guglielmo Marconi", University of Bologna, Italy
[d] Dpt. of Cardiology, Hospital Universitario Virgen de la Arrixaca de Murcia, Spain
[e] Instituto de Química Médica CSIC, Madrid, Spain
[f] Dpt. of Cardiac Electrophysiology, The Heart Hospital, Institute of Cardiovascular Science, University College London, London, UK

ARTICLE INFO

*Article history:*
Received 7 December 2016
Received in revised form 14 June 2017
Accepted 20 July 2017
Available online 22 July 2017

*Keywords:*
$K_V$7.1
KCNE1
Long QT syndrome
Electrophysiology

ABSTRACT

$K_V$7.1 and KCNE1 co-assemble to give rise to the $I_{Ks}$ current, one of the most important repolarizing currents of the cardiac action potential. Its relevance is underscored by the identification of >500 mutations in $K_V$7.1 and, at least, 36 in KCNE1, that cause Long QT Syndrome (LQTS). The aim of this study was to characterize the biophysical and cellular consequences of the D242N $K_V$7.1 mutation associated with the LQTS. The mutation is located in the S4 transmembrane segment, within the voltage sensor of the $K_V$7.1 channel, disrupting the conserved charge balance of this region. Perforated patch-clamp experiments show that, unexpectedly, the mutation did not disrupt the voltage-dependent activation but it removed the inactivation and slowed the activation kinetics of D242N $K_V$7.1 channels. Biotinylation of cell-surface protein and co-immunoprecipitation experiments revealed that neither plasma membrane targeting nor co-assembly between $K_V$7.1 and KCNE1 was altered by the mutation. However, the association of D242N $K_V$7.1 with KCNE1 strongly shifted the voltage dependence of activation to more depolarized potentials (+50 mV), hindering $I_{Ks}$ current at physiologically relevant membrane potentials. Both functional and computational analysis suggest that the clinical phenotype of the LQTS patients carrying the D242N mutation is due to impaired action potential adaptation to exercise and, in particular, to increase in heart rate. Moreover, our data identify D242 aminoacidic position as a potential residue involved in the KCNE1-mediated regulation of the voltage dependence of activation of the $K_V$7.1 channel.



## 1. Introduction

Cardiac channelopathies are responsible for about a quarter of non-ischemic sudden cardiac deaths, the most prevalent and well-known disorder within this group being the congenital Long QT syndrome (LQTS), which is more predominant in women than in men, since women exhibit a longer QT interval [1,2]. The prolonged QTc interval (usually >480 ms) in the electrocardiogram (ECG) in these patients is caused by a delayed repolarization of the cardiac action potential (AP). Such LQT intervals can cause a polymorphic ventricular tachycardia called *torsades de pointes* and, in some cases, sudden cardiac death. Fifteen genes are associated with LQTS [1]. Among all of them, the *KCNQ1* gene accounts for >30% of the identified pathological genetic variants and mutations in LQTS causing the LQTS type 1 (LQTS1). *KCNQ1* gene codifies for $K_V$7.1 channels that, after assemble with KCNE1 subunits, generate the $I_{Ks}$ current that greatly contributes to the repolarization of the cardiac AP [3–5]. Assembly with KCNE1 profoundly modifies the biophysical characteristics of the current: it slows the activation and deactivation kinetics, shifts the voltage dependence of the activation to more positive potentials, removes the inactivation, increases unitary conductance, increases $PIP_2$ sensitivity and confers sensitivity to the β adrenergic-PKA mediated activation, reconstituting the characteristics of the native cardiac $I_{Ks}$ current [6–10]. This current becomes predominant at fast cardiac rate due to its extraordinary slow activation and deactivation kinetics that lead to an accumulation of $K_V$7.1-KCNE1 channels in the activated-closed states, facilitating channel opening when it is required [11]. Accordingly,

* Corresponding authors at: Instituto de Investigaciones Biomédicas Alberto Sols, CSIC-UAM, C/Arturo Duperier 4, 28029 Madrid, Spain.
*E-mail addresses:* tgonzalez@iib.uam.es (T. Gonzalez), cvalenzuela@iib.uam.es (C. Valenzuela).
[1] Current address: Dpt. of Cardiology, Cardiovascular Research Institute Maastricht, Maastricht University Medical Centre, Maastricht, The Netherlands.
[2] Both authors equally contributed to this work.

http://dx.doi.org/10.1016/j.yjmcc.2017.07.009
0022-2828/

exercise and emotional stress trigger arrhythmias in >80% of the LQTS1 patients making evident the key role of this current during elevated heart rates [12].

In this study, we analyzed the functional consequences of the *KCNQ1* mutation D242N (chr11:2572053G > A, c.724G > A) localized in the exon 5, found in two patients (twins) with LQTS. This genetic variant has been previously identified in other genetic studies [13–18]. D242 is located in the C-terminal half of the S4 domain facing the surface boundary of the S4-S5 linker. The S4 segment is the major contributor of the voltage sensing domain, thanks to a string of charged amino acids. Here we show that D242N mutation disturbs the charge balance of the $K_V$7.1 sensor domain leading to a significant right shift of the voltage dependence of activation determined by KCNE1 interaction. Our data show that D242N $K_V$7.1-KCNE1 channels generate negligible currents at physiological membrane potentials supporting its major role in the LQTS phenotype of the patients.

## 2. Materials and methods

The institutional review board at The Heart Hospital, Institute of Cardiovascular Science (London) approved the study, and the patients provided written informed consent. The study conforms to the Declarations of Helsinki. There is an online extended Materials and Methods section.

### 2.1. Mutagenesis and cell transfection

The D242N mutation was introduced in the pEYFP-N1-*KCNQ1* by PCR using QuickChange II XL Site-Directed Mutagenesis Kit (Agilent Technologies) following manufacturer's instructions. COS7 and HEK293 cells were transiently transfected with $K_V$7.1-pEYFP (WT and/or D242N) and KCNE1-pECFP by using Fugene6 (COS7) or Metafecte™ Pro (HEK293), following the manufacturer's instructions.

### 2.2. Protein purification and western blot analysis

Twenty-four hours after transfection, HEK293 cells were washed twice with ice-cold PBS and the appropriate procedure was performed, either for biotinylation or immunoprecipitation experiments. Cell surface proteins biotinylation was carried out with Pierce Cell Surface Protein Isolation Kit (Pierce) following manufacturer's instructions. For the immunoprecipitation assay we used Protein A-Sepharose beads (GE Healthcare) that were coated with anti-KCNE1 or anti-$K_V$7.1 antibodies (Alomone Labs).

Protein samples, containing equal amounts of protein were incubated at 65 °C for 10 min in 250 mM Tris-HCl, pH 6.8, 2% SDS, 10% glycerol and 2% β-mercaptoethanol and size-separated in 8% SDS-PAGE gel. Gels were blotted onto an Immobilon-P nitrocellulose membrane (Millipore) and processed as recommended by the antibodies supplier.

### 2.3. Confocal microscopy

HeLa cells seeded on a glass coverslip were fixed 24 h after transfection of $K_V$7.1-pECFP-N1 or D242N $K_V$7.1-pECFP-N1, KCNE1-pEYFP-N1 and Akt-PH-pDsRed or pDsRed-ER. Cell preparations were imaged under Zeiss LSM 880 confocal microscope (Zeiss) equipped with an argon multiline laser (458 for pECFP, 488 and 514 nm for pEYFP) and a red light laser (DPSS 561 for pDsRed).

### 2.4. Electrophysiological recordings

Currents were recorded from transiently transfected COS7 cells using the perforated amphotericin B-patch-clamp technique with an Axopatch 200B amplifier (Axon Instruments) as described [19,20].

### 2.5. Computational analysis

To estimate the effects of the mutation in heterozygous conditions (D242N/WT $K_V$7.1-KCNE1) on the APD, the O'Hara-Rudy (ORd) model was used [21] (see supplemental methods). The effects of β-adrenergic stimulation were simulated by acting on $I_{Ks}$, $I_{CaL}$ and $I_{up}$ according to previous computational studies [22]. The pseudo-ECG signal was also computed on a one-dimensional fiber taking into account the transmural heterogeneity, as previously described [23].

### 2.6. Statistics

Data are presented as mean values ± SEM. Two-way ANOVA repetitive measurements test followed by Bonferroni test were used to assess statistical significance when appropriate. A value of $P < 0.05$ was considered significant (see online Material and methods section).

## 3. Results

### 3.1. Patient characteristics: clinical analysis and genetics

Two 20 years-old dizygotic twins (female and male) were evaluated after presenting with episodes of syncope and one nocturnal seizure pre-diagnosis. Both twins were genetically examined and it was found that they carried the *KCNQ1* mutation D242N (chr11:2572053G > A, c.724G > A) localized in the exon 5. Cardiac examination and echocardiogram were unremarkable. In both patients, the ajmaline challenge for Brugada Syndrome was normal. The sister had a clinical history of two syncopes while standing and one nocturnal seizure in childhood but an unremarkable ECG apart from a J point elevation of 0.5 mm inferior laterally and mildly prolonged QT interval at rest (QTc 473 ms). The QT interval was prolonged with exercise, reaching a maximum QTc of 527 ms (Fig. 1A, Table S1). The twin brother had a one syncopal episode following playing a computer game, normal ECG with J point elevation of 0.5 mm in inferior leads and a QTc at rest of 410 ms. With exercise he initially developed a bifid T wave which was normalized at higher heart rates and the QTc increased to 522 ms. A marked prolongation of QTc was seen at peak exercise, with rapid normalization during recovery (Fig. 1B, Table S2). An ECG from their father, aged 54 years, was available for evaluation. J point elevation of 1.5 mm in inferior, lateral leads with mild ST elevation consistent with early repolarization and mild notching in V1 were the only notable findings. QTc interval at rest was normal (421 ms). There was no family history of sudden death. An ECG from the mother was not available for evaluation.

### 3.2. Functional characterization of D242N $K_V$7.1 channels

First, we analyzed the subcellular localization of the mutant and we observed a similar pattern of trafficking between WT and D242N $K_V$7.1-CFP channels characterized by a high ER retention (Fig. 1A and B). Currents were elicited by applying 5.5 s pulses to potentials between −80 and +100 mV from a holding potential of −80 mV in 20 mV steps. The activation kinetics of mutant channels was slower than that of WT channels (Fig. 2C and D, Fig. S2). The current-voltage (I—V) relationship of D242N $K_V$7.1 showed a mild loss-of-function at membrane potentials positive to +40 mV compared to WT KV7.1 channels (Fig. 2E), without changes in the activation curve (Fig. 2F).

As it is shown in Fig. 2C, tail currents of D242N $K_V$7.1 currents did not exhibit the typical hook of WT $K_V$7.1 channels [3,4]. To analyze the voltage dependent of inactivation of WT and D242N $K_V$7.1 channels using the tail current analysis previously reported [24]. As shown in Fig. 2G, inactivation of WT $K_V$7.1 channels was evident in the hook of the tail currents recorded at −120 mV after 5.5 s depolarizing pulses to different potentials, between −60 and +100 mV. This hook is attributed to a rapid recovery from inactivation. Two components of tail currents can be measured in the tails: the instantaneous current ($I_{inst}$) and the

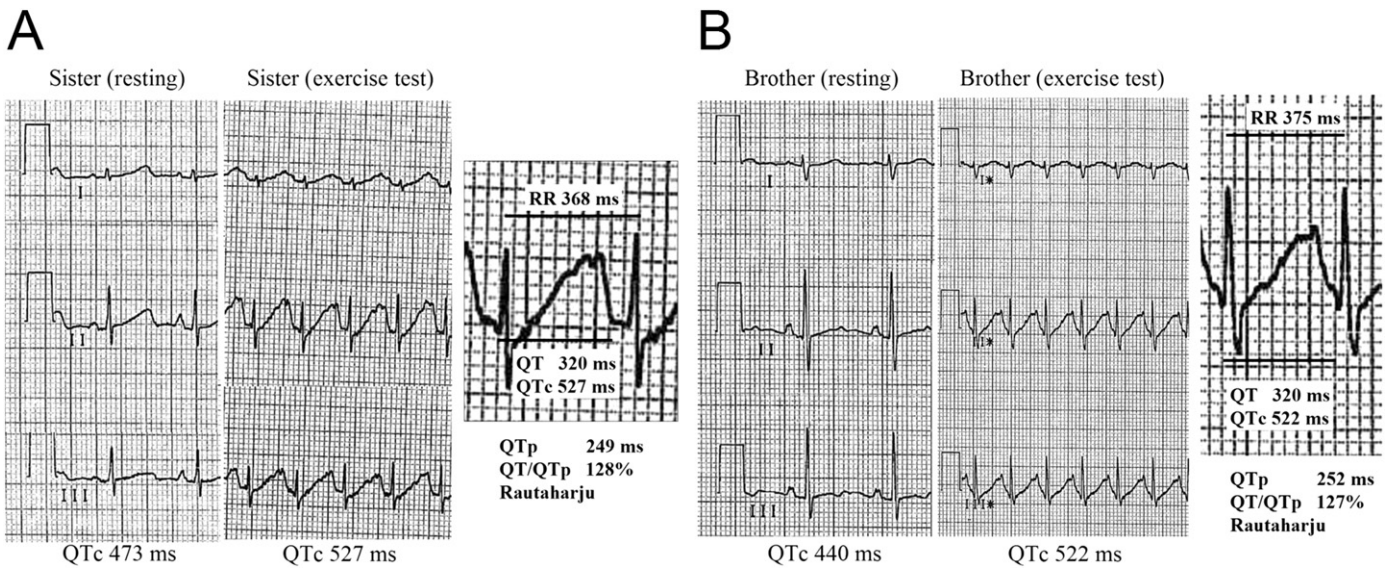


**Fig. 1.** ECGs of the patients. ECG detail (leads I, II, III) of affected twins sister (A) and brother (B) taken at baseline and peak exercise showing a significant prolongation of QT interval. Frequency QT corrected for the frequency using Bazzet (QTc) and Rautaharju methods (QTp).

extrapolated one ($I_{extrapol}$) obtained from a monoexponential fit of the tail current after the initial hook. The ratio $I_{inst}/I_{extrapol}$ was used to analyze the channel availability (Fig. 2H). The half-inactivation voltage was $-19.1 \pm 2.1$ mV ($n = 5$) in WT $K_V7.1$ channels. As observed, D242N $K_V7.1$ channels lost the inactivation.

### 3.3. Loss of function of D242N $K_V7.1$-KCNE1 channels

To investigate the effects of the D242N mutation on $K_V7.1$ currents in the physiologically relevant channel complex ($K_V7.1$-KCNE1), WT or D242N $K_V7.1$ channels were co-transfected with KCNE1 subunits in HEK293 and COS7 cells. First, we analyzed the trafficking of these complexes to the plasma membrane, which, in some mutations, explains the decrease of the current [23,25,26]. Subcellular distribution of D242N $K_V7.1$-KCNE1 resembled that of WT $K_V7.1$-KCNE1 channels (Fig. 3A and B). Also, the WT and the mutant KV7.1 channels colocalized and coimmunoprecipitated with KCNE1 to the same extent (Fig. S1A and S1B). Despite the high intracellular retention observed, the targeting of both, WT and D242N KV7.1, to the plasma membrane was further confirmed by a cell surface biotinylation assay with no major differences between them (Figs. S1A and S2B).

Secondly, we studied the electrophysiological characteristics of the D242N $K_V7.1$ channels assembled with KCNE1 subunits (Fig. 3C and D). Coexpression of the mutant channel with KCNE1 caused a dramatic current inhibition compared to WT $K_V7.1$-KCNE1. Thus, the current generated by D242N $K_V7.1$-KCNE1 channels after depolarizing from a holding potential of $-80$ mV to $+60$ mV for 5.5 s was significantly smaller than that elicited by WT $K_V7.1$-KCNE1 channels ($438.6 \pm 80.8$ pA *vs.* $2571.0 \pm 568.4$ pA in D242N and WT $K_V7.1$-KCNE1 channels, respectively, $n = 10/15$, $P < 0.01$) (Fig. 3C–E). Fig. 3F shows the activation curves obtained for WT and mutant complexes. Thus, the loss-of-function produced by the mutation seems to be due to a positive-shift of the voltage dependence of activation of $K_V7.1$-KCNE1 complex. Finally, the deactivation kinetics was faster in D242N than in WT $K_V7.1$-KCNE1 channels ($59.6 \pm 7.7$ ms *vs.* $435.8 \pm 71.7$ ms, $n = 16/10$, $P < 0.01$, Fig. 3C and D), which represents loss of function during AP repolarization.

The activity of $I_{Ks}$ is crucial for cardiac AP repolarization. More precisely, it contributes to the adaptation to heart rate changes [22,27,28]. Slow activation of $I_{Ks}$ ensures that the current activated in a single cardiac AP does not reach the maximal value and, due to its incomplete deactivation during short diastole periods, can be further increased upon repeated depolarizations, leading to a cardiac AP shortening in response to fast heart rate [29]. In order to elucidate if the rate-dependency of the $I_{Ks}$ generated by the mutant channel was modified, trains of 70 pulses to $+50$ mV, from $-80$ mV, were applied at 1, 2 and 2.5 Hz, mimicking low (resting) and fast (exercise) heart rates (Fig. 4A). As previously described, for WT $K_V7.1$-KCNE1 complexes [23], a significant increase in the current was observed at fast rates (≥2 Hz). Fig. 4B shows the current amplitude of each pulse plotted as a function of the pulse number. Thus, cells expressing D242N $K_V7.1$-KCNE1 channels, exhibited a smaller increase in the current magnitude at all frequencies tested.

### 3.4. Heterozygous condition

We mimicked the heterozygous condition of the patients reported by co-expressing WT, D242N $K_V7.1$ channels with KCNE1 (Fig. 5A). Heteromeric D242N/WT $K_V7.1$-KCNE1 channels exhibited intermediate electrophysiological characteristics between WT and mutant homomeric channels. Fig. 5B, shows the I–V relationship of the heterozygote exhibiting similar current magnitude than WT $K_V7.1$-KCNE1 channels. Fig. 5C shows the activation curves for WT/D242N $K_V7.1$-KCNE1 heteromeric channels, which exhibited a mild shift of the $V_h$ to positive potentials *vs.* WT $K_V7.1$-KCNE1 channels but smaller than homomeric D242N $K_V7.1$-KCNE1. These results indicate that the mutation has not a dominant negative effect against WT channels. Also, the deactivation kinetics was faster than in WT $K_V7.1$-KCNE1 channels ($313.8 \pm 89.2$ ms *vs.* $513.6 \pm 37.0$ ms, $n = 5/15$, $P < 0.05$), but slower than in D242N/WT $K_V7.1$-KCNE1 channels ($313.8 \pm 89.2$ ms *vs.* $59.6 \pm 7.7$ ms, $n = 5/16$, $P < 0.05$).

### 3.5. D242N mutation impairs cardiac AP rate adaptation

A human ventricular cell computer model (O'hara Rudy model) was used to examine the effects of mutant channels (D242N/WT $K_V7.1$-KCNE1, mimicking the heterozygous condition) on AP morphology in endocardial, epicardial and M cells (Fig. 6). At basal rate (60 bpm), the mutation had negligible effects for all cell types, whereas at high rate (180 bpm) and concomitant β-adrenergic stimulation (mimicking exercise conditions) the mutant AP failed to adapt its duration to the same extent than the WT one (*e.g.* 281 *vs.* 267 ms in M cells, Fig. 6A right panels), due to a smaller amount of $I_{Ks}$ current (Fig. 6A, middle panels). The impaired rate adaptation exhibited by the mutant was also

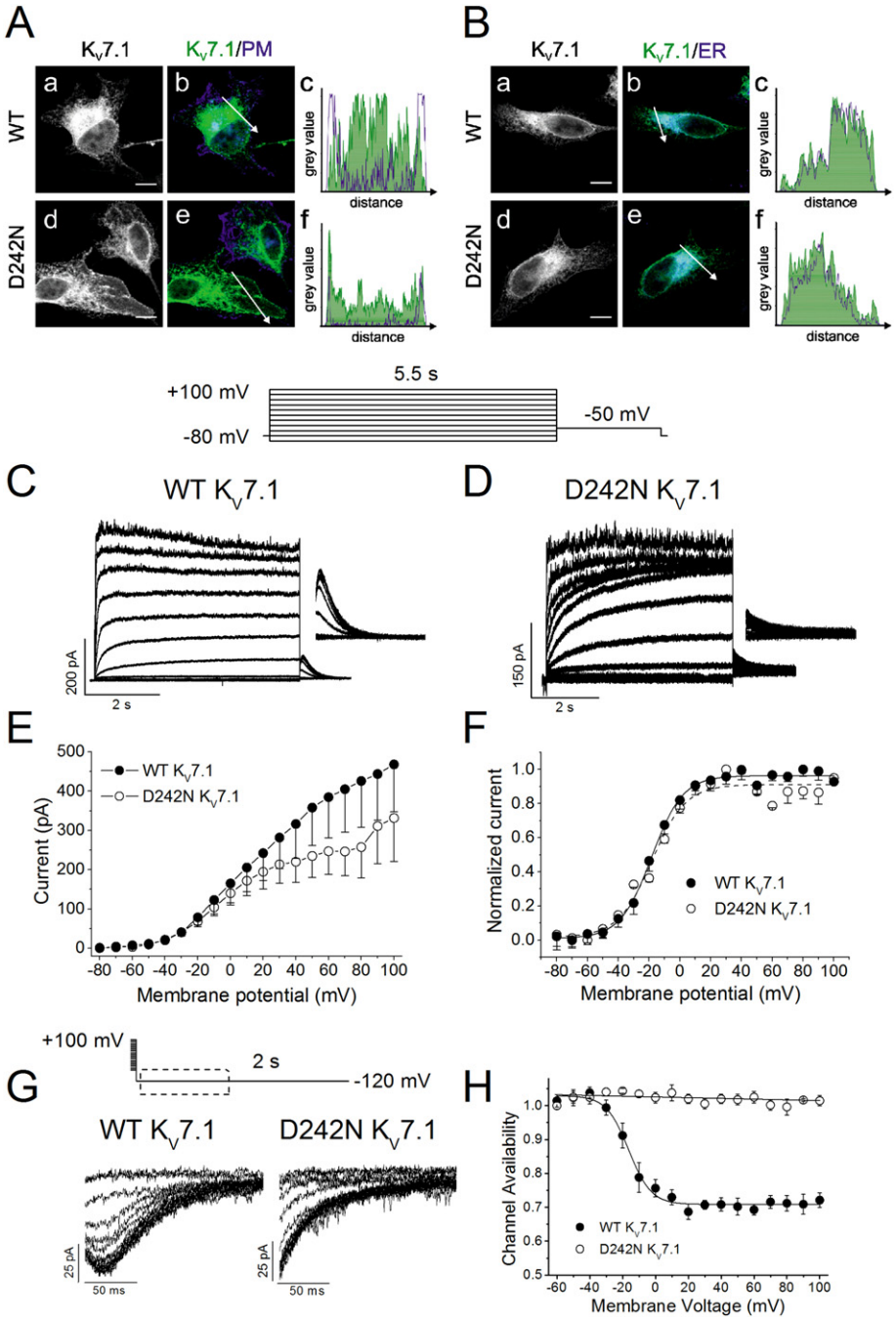


**Fig. 2.** Trafficking and characterization of D242N $K_V$7.1 channels. HeLa cells were transfected with either $K_V$7.1-CFP (WT) or D242N $K_V$7.1-CFP (D242N), and Akt-PH-pDsRed as plasma membrane (PM) marker (A) and DsRed-ER as endoplasmic reticulum (ER) marker (B). Aa–Ac WT PM surface expression. Ad–Af D242N PM surface expression. Ba–Bb WT ER retention. Bd–Be D242N ER retention. Aa, Ad, Ba and Bd show $K_V$7.1 channels, either WT or D242N, in grey scale. Ab, Ae, Bb and Be show merge images of $K_V$7.1 channels (WT or D242N) in green, and marker (PM or ER) in blue. Colocalization is highlighted in cian. Ac, Af, Bc and Bf are histograms of the pixel-by-pixel analysis of the arrow section in merge panels. Green profile corresponds to channels (WT or D242N) and blue profiles to subcellular marker (PM or ER). Scale bars, 10 μm. C and D display representative currents of WT and D242N $K_V$7.1 channels after applying the pulse protocol shown at the top of the Figure. Inset: Enlarged tail currents recorded at −50 mV. E. I–V relationships of current measured at the end of the 5.5 s depolarizing pulses for WT (black circles) and D242N $K_V$7.1 channels (white circles). E. Activation curves obtained by plotting the normalized tail currents vs. membrane potential with midpoint activation (Vh) and slope (s) values of Vh = −19.9 ± 3.2 mV, s = 11.3 ± 2.2 mV vs. Vh = −13.8 ± 4.1 mV and s = 14.7 ± 1.7 mV, for WT and D242N channels, respectively ($P > 0.05$, $n = 9/6$). G shows current traces of WT and D242N $K_V$7.1 channels obtained after applying a 3-pulse protocol shown in the top. Cells were pulsed at +40, +60, +80 and +100 mV for 2 s before applying a 20 ms interpulse at −130 mV to allow channels to recover from inactivation. The membrane potential was returned to the test potential after 20 ms to −130 mV interpulse to assess the extent of recovery. H. Plot of the degree of inactivation measured at each test potential. E, F and H, values are mean ± SEM of n = 10/5 experiments, $^{*}P < 0.05$ and $^{**}P < 0.01$.

observed by computing the rate dependence curve ($APD_{90}$ *vs.* pacing cycle length) for the three cellular types (Fig. 6C).

In order to relate the modeled changes in $APD_{90}$ to QTc (*i.e.*, to test if QTc increases at high heart rates as those observed during exercise in patients could be reproduced in simulations), pseudo-ECGs for WT/D242N $K_V$7.1-KCNE1 heterozygous conditions were computed. In Fig. S5 the results from simulations run exactly at the same heart rates experimentally recorded in twin #1 at baseline and under exercise (84 bpm *vs.* 163 bpm plus β-adrenergic stimulation) are shown. Only slight rate adaptation can be observed, and the simulated QTc was significantly prolonged from 387 ms to 493 ms, similarly to experimental recordings (Fig. S5 and Table S1).

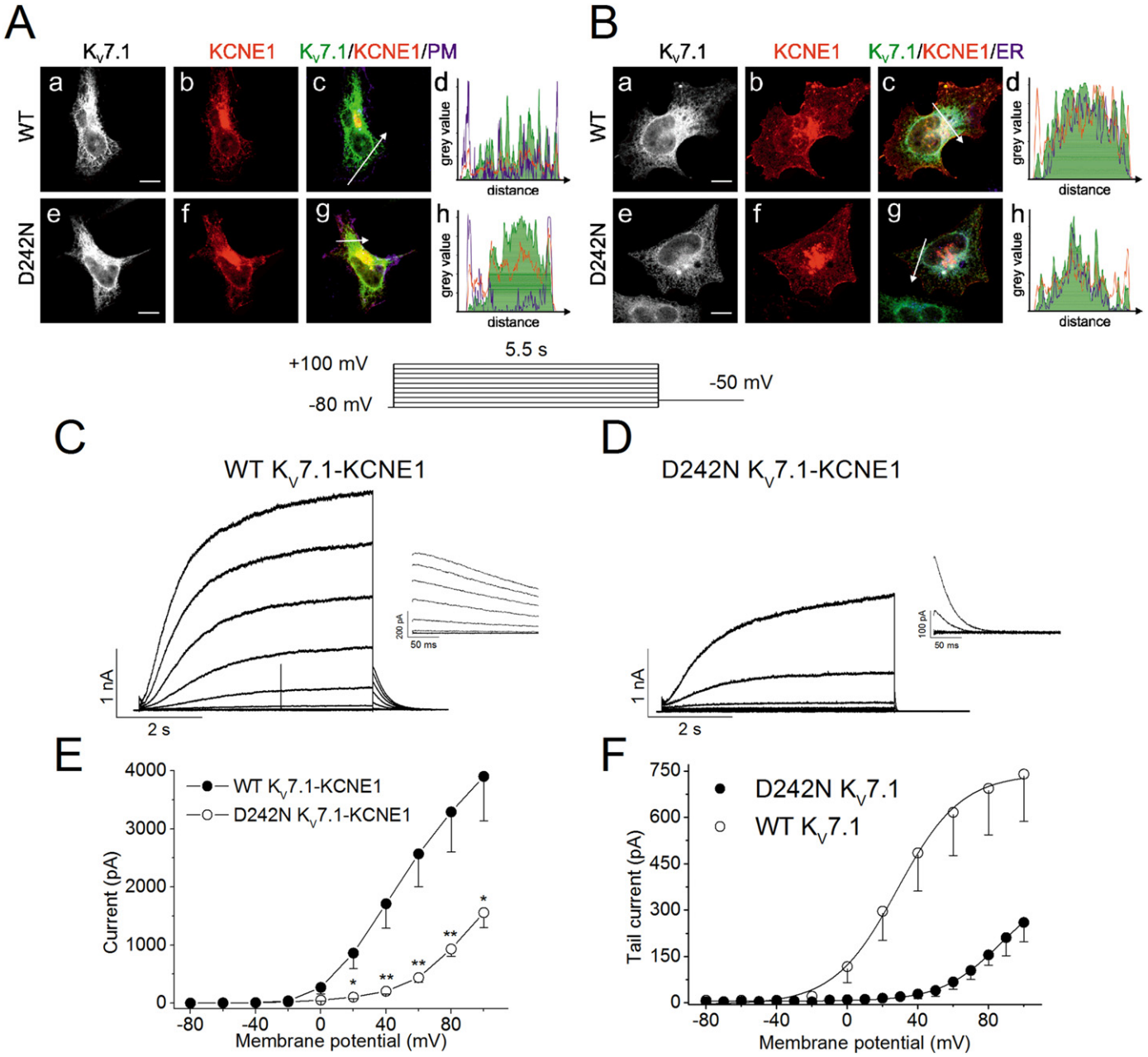


**Fig. 3.** KCNE1 produces a positive shift of D242N $K_V$7.1-KCNE1 voltage dependence of activation. HeLa cells were transfected with either $K_V$7.1-CFP (WT) or D242N $K_V$7.1-CFP (D242N), KCNE1YFP, and Akt-PH-pDsRed as PM marker and DsRed-ER as ER marker. Aa–Ad WT-KCNE1 PM surface expression. Ae–Ah D242N-KCNE1 PM surface expression. Ba–Bd WT-KCNE1 ER retention. Be–Bh D242N-KCNE1 ER retention. Aa, Ae, Ba and Be show $K_V$7.1 channels, either WT or D242N, in greys scale. Ad, Ag, Bc and Bg show marge images of $K_V$7.1 channels (WT or D242N) in green, KCNE1 in red, and subcellular marker (PM or ER) in blue. Triple colocalization in highlighted in white. Ad, Ah, Bd and Bh are histograms of pixel-by-pixel analysis of the arrow section in merge panels. Green profile corresponds to channels (WT or D242N), red profile to KCNE1 and blue profile to subcellular marker (PM or ER). Scale bars, 10 μm. Representative current traces elicited by WT $K_V$7.1-KCNE1 (A) and D242N $K_V$7.1-KCNE1 channels (B). The pulse protocol is shown at the top. C. I–V relationships after plotting the current magnitude at 5.5 *s vs.* membrane potential. D. The voltage dependence of activation obtained by plotting the tail current *vs.* membrane potential exhibited $V_h$ and *s* values of $V_h = +32.9 \pm 3.6$ mV, $s = 16.6 \pm 0.7$ mV *vs.* $V_h = +82.6 \pm 3.9$ mV ($P < 0.01$, $n = 10/13$) and $s = 13.4 \pm 1.4$ mV, for WT and D242N channels, respectively ($P > 0.05$, $n = 10/13$). Black circles: WT $K_V$7.1; white circles: D242N $K_V$7.1. Values are mean ± SEM of $n = 10/13$ experiments. $^*P < 0.05$ and $^{**}P < 0.01$.

## 4. Discussion

In this study we have characterized the LQTS-associated mutation D242N in the $K_V$7.1 channel. We observed that: 1) the affected patients carrying this mutation lost the adaptation to fast heart rate, being this effect fairly well reproduced by our computing model. 2) The voltage-dependence of D242N $K_V$7.1 channels was similar than in the WT channels, although the activation kinetics was slower and a large decrease in the inactivation was observed. 3) Neither cell surface targeting nor assembly with KCNE1 was affected. However, 4) upon co-assembly with KCNE1, the activation curve was shifted to positive potentials by 50 mV. This shift prevents D242N $K_V$7.1-KCNE1 channel opening at physiological membrane potentials. All these findings uncover the molecular mechanism of the LQTS phenotype presented by patients carrying D242N $K_V$7.1 mutation and also a $K_V$7.1 residue involved in the KCNE1-mediated voltage dependent activation of $K_V$7.1 channel.

Cell surface targeting of D242N $K_V$7.1 in the absence of KCNE1 was not affected when compared to WT $K_V$7.1 channels, thus suggesting that the electrophysiological changes observed are due to modifications in the gating of the channel and not to problems in the trafficking of the channel, as expected for a mutation in the S4 segment (main part of the voltage sensor domain of the channel). The alignment of the S4 segment

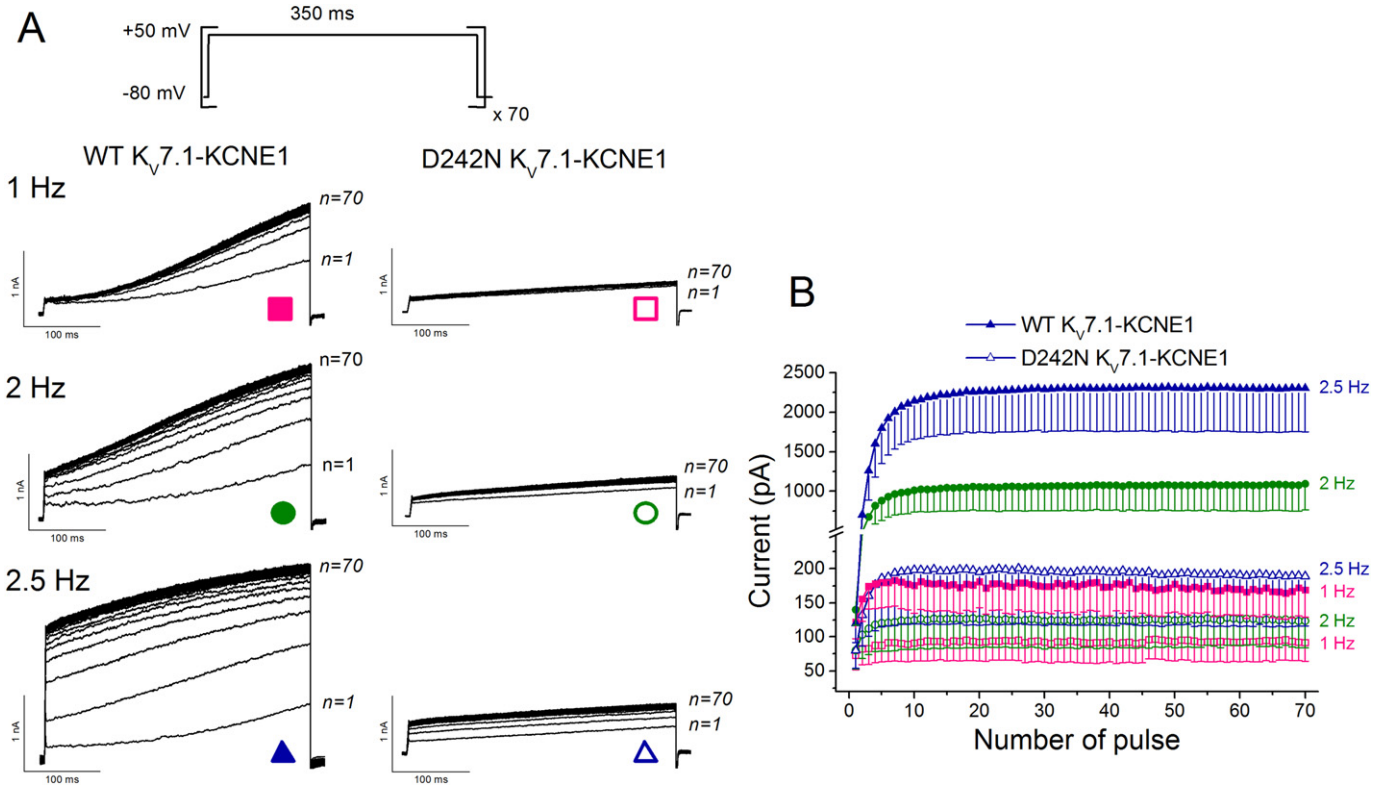


**Fig. 4.** Rate dependency of D242N $K_V$7.1-KCNE1 currents. A. Rate-dependent current increase of WT (filled symbols) and D242N (empty symbols) $K_V$7.1-KCNE1 channels at different frequencies: 1 Hz (squares), 2 Hz (circles) and 2.5 Hz (triangles). The pulse protocol consisted in 70 pulses of 350 ms in duration at different frequencies (1, 2 and 2.5 Hz) is represented at the top. B. Graph showing the instantaneous current amplitude of the pulses of each train plotted as a function of pulse number. Values are mean ± SEM of $n = 5$ experiments.

sequences of different voltage-gated channels reveals that $K_V$7.1 is unique among them. It displays an unusual paucity of net positive charges (+3) compared to other members of the voltage-gated ion channels superfamily, such as $K_V$1.1 (+7), even within $K_V$7 family (+5) (Fig. 7A). Interestingly, residue D242 is not present in other potassium channels families, which might be indicative of a particular role in $K_V$7 channels. The loss of a negative charge caused by the mutation under study, D242N, unbalances the charge equilibrium of the distal S4. But surprisingly, the voltage-dependence activation of this mutant channel was similar to that observed in WT $K_V$7.1 channels. This behavior is comparable to the effect of D242W substitution, which does not shift the voltage-dependence activation of the channel [30]. On the contrary, the D242A mutation shifts the voltage dependence of activation to negative membrane potentials and converts this channel into a

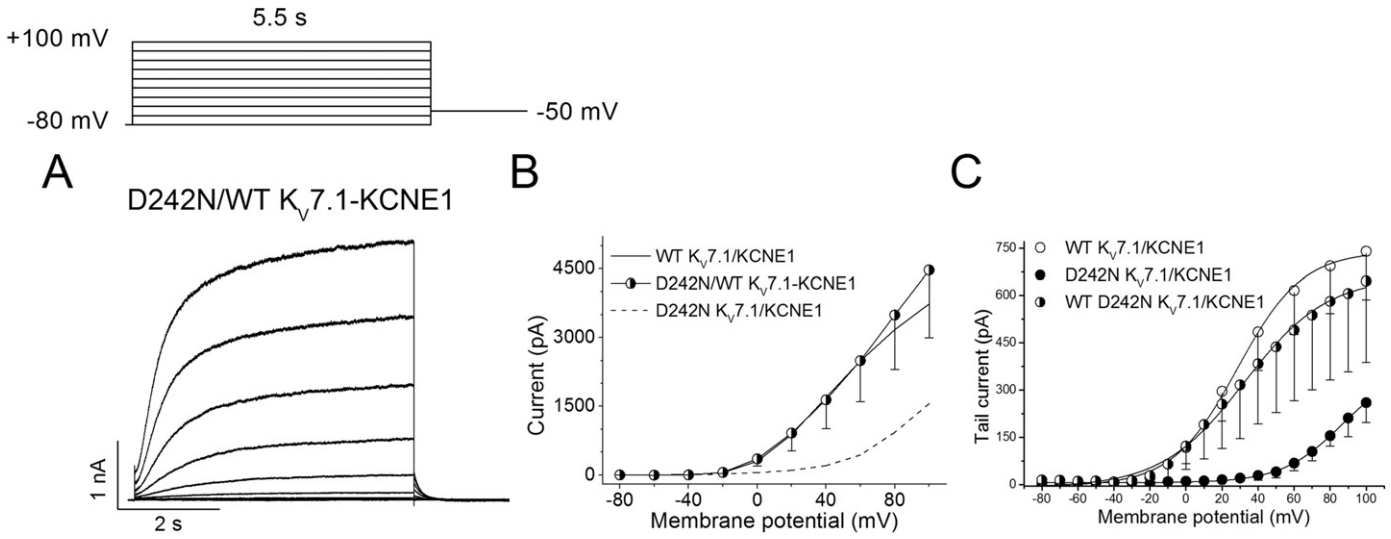


**Fig. 5.** Characteristics of the heterozygous D242N/WT $K_V$7.1-KCNE1. A. Representative traces obtained after applying the pulse protocol shown at the top. B. I–V relationship of the heterozygous condition obtained by plotting the current density at 5.5 s vs. membrane potential. The figure also shows the I–V relationships of WT $K_V$7.1-KCNE1 (solid line) and that of D242N $K_V$7.1-KCNE1 homozygous (shaded line). C. Activation curves obtained after plotting the tail current values vs. membrane potential and fit the data with a Boltzmann equation. This panel also shows the activation curves of WT $K_V$7.1-KCNE1 and that of D242N $K_V$7.1-KCNE1 homozygous. Values are mean ± SEM of n = 5 experiments.

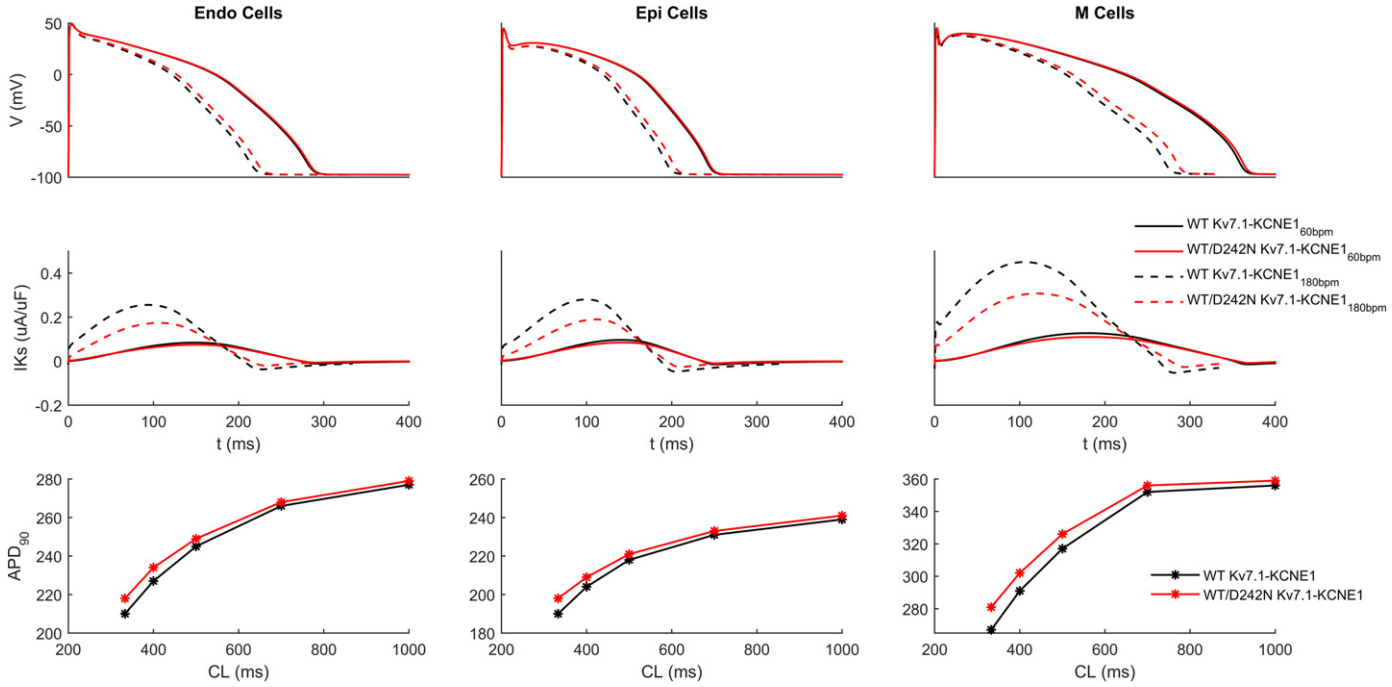


**Fig. 6.** Computational analysis of D242N/WT $K_V$7.1-KCNE1 on the ventricular AP. Comparison of ventricular APs (A), and IKs current (B) in WT $K_V$7.1-KCNE1 and D242N/WT $K_V$7.1-KCNE1 conditions for endocardial (left), epicardial (middle), and M (right) cells. Simulations were performed mimicking baseline (60 bpm) and exercise (180 bpm and β-adrenergic stimulation) conditions, using the ORd model. (C) Rate dependence curve for WT $K_V$7.1-KCNE1 (black) and D242N/WT $K_V$7.1-KCNE1 (red) simulating the effect of exercise at the cellular level (no β-adrenergic stimulation at CL = 1000 ms, 25% of β-adrenergic stimulation at CL = 700 ms, 50% of β-adrenergic stimulation at CL = 500 ms, 75% of β-adrenergic stimulation at CL = 400 ms and 100% of β-adrenergic stimulation at CL = 333 ms).

constitutively open channel [31]. These data suggest that residue volume might be more important than the charge at this position. On the other hand, D242N $K_V$7.1 current exhibited slower activation kinetics and a decreased inactivation, confirming the functional role of S4 in the channel gating [31,32].

The charge paucity of the C-terminal half of the S4 domain has been proposed to underlie the susceptibility of $K_V$7.1 to exhibit different behaviors upon KCNE interaction [31]. Co-assembly of D242N $K_V$7.1 and KCNE1 subunits markedly shifted the voltage dependence of activation to positive potentials by 50 mV and thus, at physiological membrane potentials (from −20 to +20 mV), the currents elicited by the mutant complexes were negligible producing the delayed repolarization observed in LQTS patients carrying the D242N mutation. It has been described that D242W $K_V$7.1-KCNE1 complexes also expressed currents of small magnitude compared to WT $K_V$7.1-KCNE1, which was attributed to a low membrane expression of the complex [30]. However, here we show that D242N $K_V$7.1-KCNE1 complexes are localized in the cell membrane and their assembly with this beta-subunit is not modified *vs.* WT $K_V$7.1-KCNE1. The D242A mutation did not produce significant effects on the voltage dependence when the channel was assembled with KCNE1 subunits [31]. Based on these data, it is unlikely that the effect of D242N mutation can be attributed solely to the negative charge lost. It is worthwhile to consider residues M238 and L239, in the S4 segment, that according to Smith's model [33] are in the proximity of D242 (Fig. 7B). Mutations of these residues to the more voluminous tryptophan generated very small currents only in the presence of KCNE1, which suggested that these residues might pack tightly when the channel assemble with KCNE1 [30]. Moreover, mutation of two phenylalanines that have been predicted to be involved in the modulation of $K_V$7.1 channels by KCNE1 (F232 in S4 and F279 in S5) to different amino acids, produced a clear side-chain volume-dependent shift in the midpoint of the activation curve when the channels were expressed together with KCNE1 [23,34]. Thus, it might be hypothesized that the slight increase in volume from aspartic to asparagine [35] and/or the presence of a polar uncharged residue might modify the packing environment between D242N $K_V$7.1 and KCNE1. The rearrangement of the WT $K_V$7.1 channel in the presence of KCNE1 induces a positive shift in the activation curve of the channel [4]. D242N is boosting this feature, either by stabilizing the resting state of the channel or by destabilizing the activated state. In fact, deactivation kinetics is much faster in D242N $K_V$7.1-KCNE1 than in WT $K_V$7.1-KCNE1 channels by about 10-fold. These data highlights the importance of D242 in the fine-tuning modulation of $K_V$7.1 activity by the KCNE1 subunit.

The potassium current generated by the heteromeric D242N/WT $K_V$7.1-KCNE1 channels exhibited a similar magnitude and activation kinetics than WT $K_V$7.1-KCNE1 channels, likely due to the mild shift in the voltage-dependence of activation induced by this mutation. However, the deactivation kinetics of the current generated by these complexes remained faster than WT $K_V$7.1-KCNE1, which may affect the fast heart rate adaptation. These results suggest that, in cardiomyocytes, this mutation would induce a delay in the repolarization phase of the cardiac AP. This effect ultimately triggers the observed prolongation of the QT interval detected in D242N-LQTS1 patients and an almost complete loss of the adaptation to high heart rates. This result may be attributed to the acceleration of the deactivation kinetics observed in the D242N/WT $K_V$7.1-KCNE1 channels; since the contribution of $I_{Ks}$ to the AP repolarization is rate dependent [28] and the channels accumulate in the pre-open states, which leads to a rate-dependent increase of current, causing AP shortening [22,36]. Our results suggest that this mutation, also in heterozygous, favors the closed state of the channel, which indicates that they cannot properly respond to heart rate changes like WT $K_V$7.1-KCNE1 channels. The two symptomatic twins with a confirmed diagnosis of LQTS1, by clinical and genetic studies, were recommended with beta-blockers and they did not exhibit recurrences of syncope during a 10 years follow-up, thus confirming that this mutation in heterozygous is mostly relevant under β-adrenergic stimulation (*i.e.*, during exercise).

Our computational analysis fully confirmed this interpretation and provided a plausible explanation for the clinical manifestations of the mutation with a slight decrease in the QT interval during exercise, but

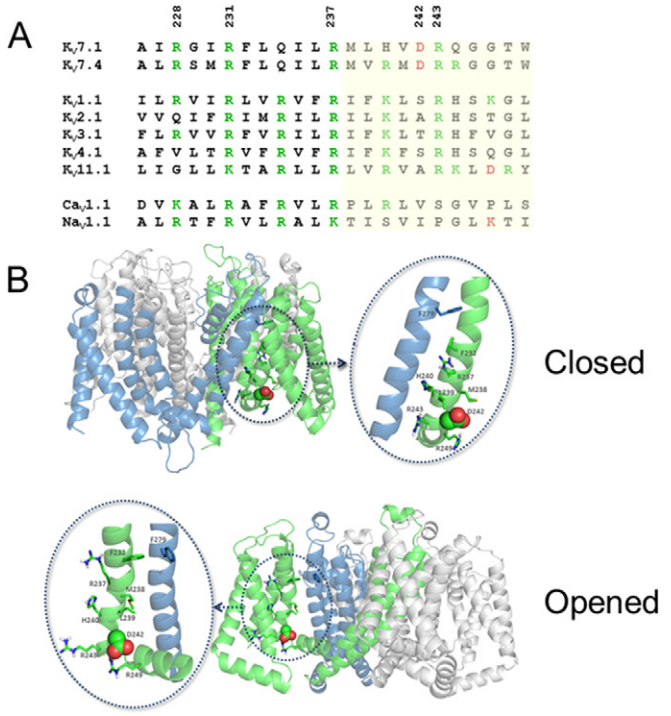


**Fig. 7.** The C-terminal of S4 segment of $K_V7.1$ is unique among voltage-gated ion channels. A. Amino acid sequence alignment of $K_V7.1$ transmembrane S4 domain with $K_V7.4$, another member of the $K_V7$ family and other representative members of the voltage-gated potassium channel subfamilies ($K_V1.1$, $K_V2.1$, $K_V3.1$, $K_V4.1$ and $K_V11.1$) and voltage-gated ion channel superfamily ($Ca_V1.1$ and $Na_V1.1$). The positions of S4 charged residues in KV7.1 are indicated at the top. Positively and negatively charged residues are colored in green and in red, respectively. The COOH-half region of every voltage-gated ion channel is highlighted in yellow. B. Cartoon representation of the closed (top) and opened (bottom) states of $K_V7.1$ channel based on the Smith et al. model [33]. Side view with the extracellular solution above and the intracellular media below. Only two monomers are colored in blue and green for better visualization. The D242 residue is indicated by spheres surrounded by residues in stick representation. Only polar hydrogens are shown. The PyMOL Molecular Graphics System, Version 1.7 Schrödinger, LLC was used.

a great increase in the QTc. While the mutation has negligible effects on the action potential at baseline, a failure to adapt to exercise conditions was identified (see Fig. 6A and Fig. S5). At the cardiomyocyte level, the $I_{Ks}$ current amplitude increases with heart rate and β-adrenergic stimulation. In our simulation model, we were able to separately quantify the effects of these two main factors participating to exercise adaptation. Our simulation results suggest that both factors equally contribute since if rate is increased with no β-adrenergic stimulation, a small decrease in APD adaptation is observed (*e.g.* WT: from 356 to 298 ms, D242N/WT: from 359 to 305 ms, at 180 bpm) and a similar effect is produced by simulation of β-adrenergic stimulation alone with no change in rate (WT: from 298 to 267 ms, D242N/WT: from 305 to 281 ms).

## 5. Conclusion

We provide evidence that the D242N $K_V7.1$ mutation exhibits a loss-of-function when associated with KCNE1 regulatory subunits and that the decrease in the current is caused by a positive shift of 50 mV in the activation curve rather than trafficking defects. The patients carrying this mutation lost the adaptation to fast heart rate, being this effect fairly well reproduced by our computing model.

## Disclosures

None.

## Acknowledgments

This work was supported by Ministerio de Economía y Competitividad (MINECO) Spain (SAF2013-45800-R, SAF2016-75021-R, BFU2014-54928-R, RIC RD12/0042/0019 and CIBER CB/11/00222). PDL is supported by UCLH Biomedicine NIHR. The cost of this publication was paid in part by funds from the European Fund for Economic and Regional Development. TG holds a Ramón y Cajal contract. AdlC and DAP held CSIC contracts.

## Appendix A. Supplementary data

Supplementary data to this article can be found online at http://dx.doi.org/10.1016/j.yjmcc.2017.07.009.

## References

[1] S.G. Priori, A.A. Wilde, M. Horie, Y. Cho, E.R. Behr, C. Berul, et al., HRS/EHRA/APHRS expert consensus statement on the diagnosis and management of patients with inherited primary arrhythmia syndromes: document endorsed by HRS, EHRA, and APHRS in May 2013 and by ACCF, AHA, PACES, and AEPC in June 2013, Heart Rhythm. 10 (2013) 1932–1963.
[2] C. Valenzuela, Female gender: risk factor for congenital long QT-related arrhythmias, Cardiovasc. Res. 95 (2012) 263–264.
[3] J. Barhanin, F. Lesage, E. Guillemare, M. Fink, M. Lazdunski, G.K. Romey, (V)LQT1 and lsK (minK) proteins associate to form the I(Ks) cardiac potassium current, Nature 384 (1996) 78–80.
[4] M.C. Sanguinetti, M.E. Curran, A. Zou, J. Shen, P.S. Spector, D.L. Atkinson, et al., Coassembly of K(V)LQT1 and minK (IsK) proteins to form cardiac I(Ks) potassium channel, Nature 384 (1996) 80–83.
[5] Q. Wang, M.E. Curran, I. Splawski, T.C. Burn, J.M. Millholland, T.J. VanRaay, et al., Positional cloning of a novel potassium channel gene: KVLQT1 mutations cause cardiac arrhythmias, Nat. Genet. 12 (1996) 17–23.
[6] G. Romey, B. Attali, C. Chouabe, I. Abitbol, E. Guillemare, J. Barhanin, et al., Molecular mechanism and functional significance of the MinK control of the KvLQT1 channel activity, J. Biol. Chem. 272 (1997) 16713–16716.
[7] Y. Li, M.A. Zaydman, D. Wu, J. Shi, M. Guan, B. Virgin-Downey, et al., KCNE1 enhances phosphatidylinositol 4,5-bisphosphate (PIP2) sensitivity of IKs to modulate channel activity, Proc. Natl. Acad. Sci. U. S. A. 108 (2011) 9095–9100.
[8] M. Tristani Firouzi, M.C. Sanguinetti, Voltage-dependent inactivation of the human K+ channel KvLQT1 is eliminated by association with minimal K+ channel (minK) subunits, J. Physiol. Lond. 510 (1998) 37–45.
[9] M. Pusch, Increase of the single-channel conductance of KvLQT1 potassium channels induced by the association with minK, Pflugers Arch. 437 (1998) 172–174.
[10] H.S. Wang, B.S. Brown, D. McKinnon, I.S. Cohen, Molecular basis for differential sensitivity of KCNQ and I(Ks) channels to the cognitive enhancer XE991, Mol. Pharmacol. 57 (2000) 1218–1223.
[11] P.G. Volders, M. Stengl, J.M. van Opstal, U. Gerlach, R.L. Spatjens, J.D. Beekman, et al., Probing the contribution of IKs to canine ventricular repolarization: key role for beta-adrenergic receptor stimulation, Circulation 107 (2003) 2753–2760.
[12] P.J. Schwartz, S.G. Priori, C. Spazzolini, A.J. Moss, G.M. Vincent, C. Napolitano, et al., Genotype-phenotype correlation in the long-QT syndrome: gene-specific triggers for life-threatening arrhythmias, Circulation 103 (2001) 89–95.
[13] T. Itoh, T. Tanaka, R. Nagai, K. Kikuchi, S. Ogawa, S. Okada, et al., Genomic organization and mutational analysis of KVLQT1, a gene responsible for familial long QT syndrome, Hum. Genet. 103 (1998) 290–294.
[14] I. Splawski, J. Shen, K.W. Timothy, M.H. Lehmann, S. Priori, J.L. Robinson, et al., Spectrum of mutations in long-QT syndrome genes. KVLQT1, HERG, SCN5A, KCNE1, and KCNE2, Circulation 102 (2000) 1178–1185.
[15] D.J. Tester, M.L. Will, C.M. Haglund, M.J. Ackerman, Compendium of cardiac channel mutations in 541 consecutive unrelated patients referred for long QT syndrome genetic testing, Heart Rhythm. 2 (2005) 507–517.
[16] A.J. Moss, W. Shimizu, A.A. Wilde, J.A. Towbin, W. Zareba, J.L. Robinson, et al., Clinical aspects of type-1 long-QT syndrome by location, coding type, and biophysical function of mutations involving the KCNQ1 gene, Circulation 115 (2007) 2481–2489.
[17] J.D. Kapplinger, D.J. Tester, B.A. Salisbury, J.L. Carr, C. Harris-Kerr, G.D. Pollevick, et al., Spectrum and prevalence of mutations from the first 2,500 consecutive unrelated patients referred for the FAMILION long QT syndrome genetic test, Heart Rhythm. 6 (2009) 1297–1303.
[18] C. Jons, A.J. Moss, C.M. Lopes, S. McNitt, W. Zareba, I. Goldenberg, et al., Mutations in conserved amino acids in the KCNQ1 channel and risk of cardiac events in type-1 long-QT syndrome, J. Cardiovasc. Electrophysiol. 20 (2009) 859–865.
[19] A. Macias, C. Moreno, J. Moral-Sanz, A. Cogolludo, M. David, M. Alemanni, et al., Celecoxib blocks cardiac Kv1.5, Kv4.3 and Kv7.1 (KCNQ1) channels: effects on cardiac action potentials, J. Mol. Cell. Cardiol. 49 (2010) 984–992.
[20] C. Moreno, A. de la Cruz, A. Oliveras, S.R. Kharche, M. Guizy, N. Comes, et al., Marine n-3 PUFAs modulate IKs gating, channel expression, and location in membrane microdomains, Cardiovasc. Res. 105 (2015) 223–232.
[21] T. O'Hara, L. Virag, A. Varro, Y. Rudy, Simulation of the undiseased human cardiac ventricular action potential: model formulation and experimental validation, PLoS Comput. Biol. 7 (2011), e1002061.

[22] S. Severi, C. Corsi, M. Rocchetti, A. Zaza, Mechanisms of beta-adrenergic modulation of I(Ks) in the guinea-pig ventricle: insights from experimental and model-based analysis, Biophys. J. 96 (2009) 3862–3872.
[23] C. Moreno, A. Oliveras, A. de la Cruz, C. Bartolucci, C. Munoz, E. Salar, et al., A new KCNQ1 mutation at the S5 segment that impairs its association with KCNE1 is responsible for short QT syndrome, Cardiovasc. Res. 107 (2015) 613–623.
[24] M. Tristani-Firouzi, M.C. Sanguinetti, Voltage-dependent inactivation of the human K+ channel KvLQT1 is eliminated by association with minimal K+ channel (minK) subunits, J. Physiol. Lond. 510 (1998) 37–45.
[25] S. Dahimene, S. Alcolea, P. Naud, P. Jourdon, D. Escande, R. Brasseur, et al., The N-terminal juxtamembranous domain of KCNQ1 is critical for channel surface expression: implications in the Romano-Ward LQT1 syndrome, Circ. Res. 99 (2006) 1076–1083.
[26] M. Dvir, R. Strulovich, D. Sachyani, C.I. Ben-Tal, Y. Haitin, C. Dessauer, et al., Long QT mutations at the interface between KCNQ1 helix C and KCNE1 disrupt I(KS) regulation by PKA and PIP(2), J. Cell Sci. 127 (2014) 3943–3955.
[27] P.C. Viswanathan, R.M. Shaw, Y. Rudy, Effects of $I_{Kr}$ and $I_{Ks}$ heterogeneity on action potential duration and its rate dependence: a simulation study, Circulation 99 (1999) 2466–2474.
[28] M. Rocchetti, A. Besana, G.B. Gurrola, L.D. Possani, A. Zaza, Rate dependency of delayed rectifier currents during the guinea-pig ventricular action potential, J. Physiol. 534 (2001) 721–732.
[29] J. Chen, R. Zheng, Y.F. Melman, T.V. McDonald, Functional interactions between KCNE1 C-terminus and the KCNQ1 channel, PLoS One 4 (2009) e5143.
[30] D. Wu, H. Pan, K. Delaloye, J. Cui, KCNE1 remodels the voltage sensor of Kv7.1 to modulate channel function, Biophys. J. 99 (2010) 3599–3608.
[31] G. Panaghie, G.W. Abbott, The role of S4 charges in voltage-dependent and voltage-independent KCNQ1 potassium channel complexes, J. Gen. Physiol. 129 (2007) 121–133.
[32] L. Franqueza, M. Lin, I. Splawski, M.T. Keating, M.C. Sanguinetti, Long QT syndrome-associated mutations in the S4-S5 linker of KvLQT1 potassium channels modify gating and interaction with minK subunits, J. Biol. Chem. 274 (1999) 21063–21070.
[33] J.A. Smith, C.G. Vanoye, A.L. George Jr., J. Meiler, C.R. Sanders, Structural models for the KCNQ1 voltage-gated potassium channel, Biochemist 46 (2007) 14141–14152.
[34] K. Nakajo, Y. Kubo, Steric hindrance between S4 and S5 of the KCNQ1/KCNE1 channel hampers pore opening, Nat. Commun. 5 (2014) 4100.
[35] J. Tsai, R. Taylor, C. Chothia, M. Gerstein, The packing density in proteins: standard radii and volumes, J. Mol. Biol. 290 (1999) 253–266.
[36] J. Silva, Y. Rudy, Subunit interaction determines IKs participation in cardiac repolarization and repolarization reserve, Circulation 112 (2005) 1384–1391.